

Development of Robust Gold Nanoparticle Samples for
Bragg Coherent Diffraction Imaging at Modern Beamlines with Increased X-ray Flux

Landon Schnebly

A senior thesis submitted to the faculty of
Brigham Young University
in partial fulfillment of the requirements for the degree of
Bachelor of Science

Richard Sandberg, Advisor

Department of Physics and Astronomy
Brigham Young University

Copyright © 2023 Landon Schnebly

All Rights Reserved

ABSTRACT

Development of Robust Gold Nanoparticle Samples for Bragg Coherent Diffraction Imaging at Modern Beamlines with Increased X-ray Flux

Landon Schnebly

Department of Physics and Astronomy, BYU
Bachelor of Science

We seek to characterize strain across grain boundaries in polycrystalline metals using Bragg Coherent Diffraction Imaging. For this technique, we use synchrotron radiation from the Advanced Photon Source at Argonne National Laboratory to gather diffraction data from single grains and use an iterative algorithm to reconstruct 3D strain maps. Isolated patches of gold nanoparticles have proven to be ideal for BCDI. However, with the increasing x-ray flux at newer facilities, traditional dewetted crystals on silicon are proving to be less robust with the gold particles drifting due to the radiation pressure of the x-ray beam. Using the processes of photolithography, thermal evaporation, and annealing, we have developed a robust sample preparation recipe for isolated clusters of gold nanoparticles on a niobium-doped strontium titanate substrate. The resulting Au on Nb:SrTiO₃ sample has allowed us to efficiently collect reliable diffraction data during our x-ray beamtimes at the Advanced Photon Source. With these advances in sample design, we have achieved the first 3D strain map reconstructions of twin-grain boundaries using this technique.

Keywords: Bragg Coherent Diffraction Imaging (BCDI), synchrotron, beamline, radiation pressure, polycrystalline metal, gold nanoparticles, photolithography, thermal deposition, annealing, strain, grain boundaries, Scanning Electron Microscopy, Electron Backscatter Diffraction (EBSD)

ACKNOWLEDGMENTS

I would first like to acknowledge funding for this project from the DOE Office of Science Grant DE-SC0022133 and from the BYU College of Physical and Mathematical Sciences. I would also like to acknowledge the support of Richard Sandberg who served not only as my research advisor but also as a mentor and friend throughout the process. Additionally, I would like to thank all the members of my research group here at Brigham Young University as well as our collaborators at Carnegie Mellon University and at Argonne National Laboratory. We are especially thankful to the Advanced Photon Source at Argonne National Laboratory for use of the 34ID-C beamline. A special thanks also to the BYU Electron Microscopy Facility and the BYU Cleanroom Facility for providing training and access to their tools. Thanks also to Nick Allen for helping me get started in the cleanroom and for his annealing advice. Finally, I would like to thank my family, especially my wife, for supporting me through my research and academic efforts.

Contents

Table of Contents	vii
List of Figures	ix
1 Introduction	1
1.1 Motivation: Making Stronger Metals	2
1.2 Overview of Bragg Coherent Diffraction Imaging	3
1.3 Why Nanoparticles are Ideal	5
1.4 The Radiation Pressure Problem	6
1.5 Finding Grain Orientations	8
2 Methods and Sample Recipe	11
2.1 Sample Design	11
2.2 Photolithography	13
2.3 Thermal Deposition	14
2.4 Annealing	15
3 Results	17
3.1 Isolated Patches of Faceted Particles	17
3.2 Conductive Substrate and EBSD	19
3.3 Twin Grain Reconstruction	20
3.4 Conclusions	21
Appendix A Photolithography on Nb:SrTiO₃ Standard Operating Procedures	23
Appendix B EBSD of Gold Nanoparticles Standard Operating Procedures	29
Bibliography	37
Index	41

List of Figures

1.1	Microstructure of a Polycrystalline Metal	3
1.2	Bragg Coherent Diffraction Imaging Schematic	4
1.3	Bragg Peak with Alien	5
1.4	Drift during Bragg Peak Collection	7
1.5	Radiation Pressure	8
1.6	Electron Backscatter Diffraction Schematic	9
1.7	EBSD Charging Defects	10
2.1	Photolithography Mask Design	12
2.2	Photolithography Schematic	14
2.3	Thermal Deposition Schematic	15
2.4	Annealing Schematic	16
3.1	Faceted Gold Nanoparticles	18
3.2	Twin Grain Boundary Schematic	18
3.3	EBSD Comparison between Substrates	19
3.4	Twin Grain Reconstruction	20

Chapter 1

Introduction

Our research aims to investigate the fundamental properties of metals at the nanoscale using Bragg Coherent Diffraction Imaging (BCDI). In this thesis, I will present the results of my contribution to this research project, which involved participating in eight beamtimes at the Advanced Photon Source either in-person or virtually. During this time, I designed a photolithography mask, developed sample preparation procedures, and used Scanning Electron Microscopy to identify optimal experiment sites. Additionally, I contributed to the training of three undergraduate students who have since taken on these tasks. I generated all of the graphics presented in this thesis, with the exception of those noted otherwise. Furthermore, my work has resulted in co-authorship of a forthcoming paper titled "Mapping nanocrystal orientations via scanning Laue diffraction microscopy for multi-peak Bragg coherent diffraction imaging." We also anticipate including the findings outlined in this thesis in a future research publication.

In this introductory chapter, I will explain the motivation behind our research, describe our technique, and discuss the three main challenges which we have faced with previous samples: aliens, drift, and charging. These challenges highlight the importance of developing a robust sample that will enable us to obtain high-quality data and interpret it with confidence.

1.1 Motivation: Making Stronger Metals

Cars, bridges, pipes, and building infrastructures are just a few examples of metals that we depend on every day. Despite their strength, metals can fail, sometimes with catastrophic results. These macroscopic failures begin as microfractures and before that as nanoscale strain caused by imperfections in the ordered atomic structure of a metal. We seek to measure this strain to learn more about how metals begin to break and how strain begins to propagate. This understanding will help us improve metal strength and prevent metal failure through defect engineering [1].

The type of strain which we seek to measure within metals is called lattice strain. Lattice strain refers to the deformation of a crystal lattice due to the presence of defects, such as dislocations or voids, or due to external forces, such as applied stress. A crystal lattice is a material-specific repeating pattern of atomic planes that minimizes the potential energy of any given atom in the structure. Deviations from this pattern are what create strain in a single crystal.

Metals are polycrystalline materials, which means they have a microstructure consisting of small interlocking crystals called grains (see Figure 1.1). Each grain has a different orientation of crystal lattice, which means that planes of atoms do not line up for neighboring grains even though the lattice parameters are the same. The regions between grains are called grain boundaries. Grain boundaries have a large effect on the strength of metal because they prevent dislocations from propagating due to the differences in crystal structure on either side [1].

Because they cannot easily cross over the grain boundary, defects produce strain across a grain boundary. The strain across a grain boundary can be quantified by measuring the lattice spacing in each of the adjacent grains and comparing the values [2]. To measure the lattice spacing, we use Bragg Coherent Diffraction Imaging (BCDI), as described in the next section. Our eventual goal is to measure and analyze the strain across a grain boundary while under stress, to provide insights into how defects begin to propagate across grain boundaries.

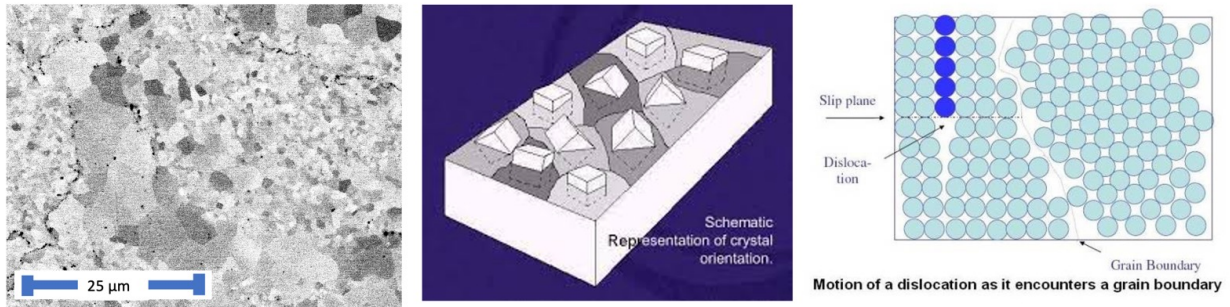


Figure 1.1 The microstructure of a metal. From left to right: Backscatter electron image showing grains in a piece of 14YWT steel represented by different levels of grayscale, schematic representation of grain orientations in a metal [3], schematic representation of a dislocation at a grain boundary [4].

1.2 Overview of Bragg Coherent Diffraction Imaging

Bragg Coherent Diffraction Imaging (BCDI) is a lensless imaging technique involving the interaction between a coherent x-ray beam and a crystalline sample and the measurement of a diffraction peak at the Bragg angle (see Figure 1.2). This technique depends on the relationship described by Bragg's Law, which relates the wavelength of the light and the spacing between planes of atoms in a crystal to the location of a peak of constructive interference:

$$n\lambda = 2d\sin(\theta_B) \quad (1.1)$$

where n is an integer, λ is the wavelength of the x-ray, d is the lattice spacing, and θ_B is the Bragg angle where a diffraction peak can be observed. Because deviations from the normal lattice spacing affect this relationship, measuring a Bragg diffraction peak provides information about strain. The use of Bragg peak diffraction data to image a crystalline grain with its three-dimensional strain field has been established [5–7]. To achieve this, the entire 3D diffraction pattern must be measured. Using knowledge about the general orientation of the crystal, we locate a Bragg peak with the detector and then allow the detector to rock through a small range of angles to collect the entire 3D diffraction pattern in detection space, also commonly referred to as reciprocal space.

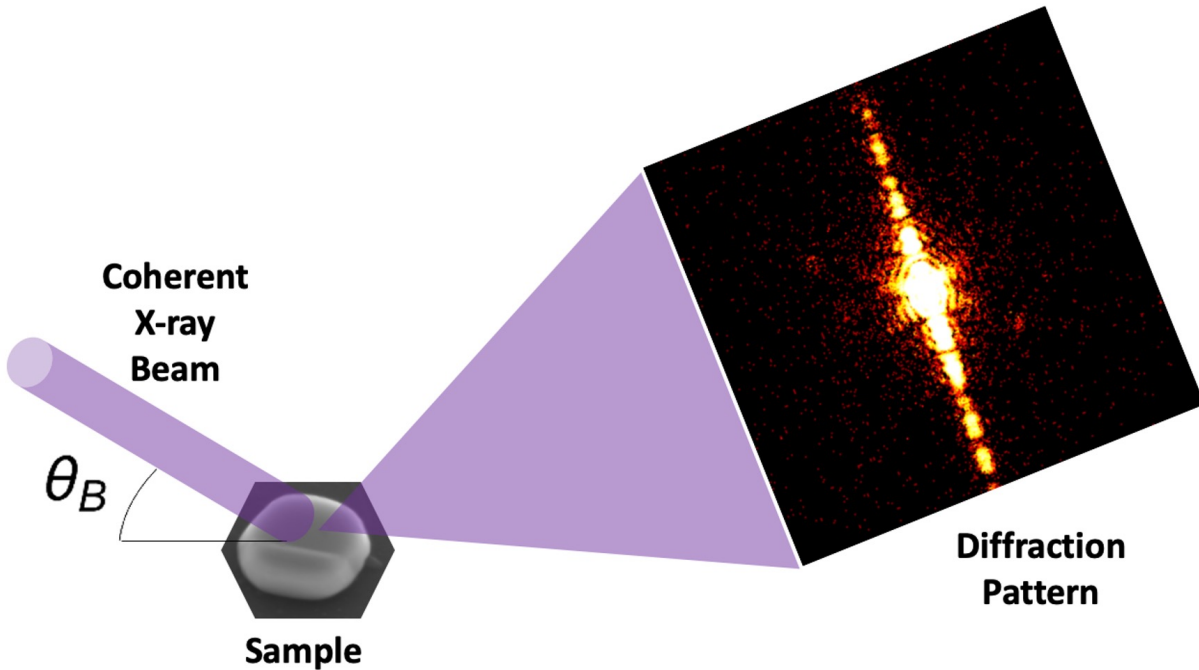


Figure 1.2 Schematic of the process we use to gather data for Bragg Coherent Diffraction Imaging

For our experiment, we used coherent synchrotron radiation from the 34ID-C beamline at Argonne National Laboratory's Advanced Photon Source to gather x-ray diffraction data. Once the entire diffraction pattern was measured, we applied iterative phase-retrieval algorithms to retrieve the 3D strain map of the original sample. For these reconstructions, we used the Cohere code developed by Barbara Frosik and Ross Harder [8]. This code iterates between real and reciprocal space using Fourier transforms, applying known constraints in real space and the collected data in reciprocal space, to converge on a solution by applying user-specified iterations of established algorithms such as error reduction and hybrid input-output [9].

1.3 Why Nanoparticles are Ideal

When acquiring diffraction data from a single Bragg peak produced by a grain within a typical polycrystalline metal structure (see Figure 1.1), we often have intruding information from a nearby grain. This is because all Bragg peaks exist in the same 3D reciprocal space. When measuring a Bragg peak, we hope to measure an area with the detector free from any other diffraction. However, information from a Bragg peak produced by a nearby grain may exist in the same region of space and show up as extra information in our scan. We call this extra information an "alien."

Aliens make it harder for our image reconstruction algorithm to converge to a solution. While Cohere does have functionalities for dealing with aliens, they involve excluding data in certain pixel areas for a given range of frames [8]. Thus, we can lose some of the intended Bragg peak data as well when we exclude the aliens, depending on their relative location to the measured Bragg peak. For example, notice the proximity of the alien in Figure 1.3 to the main pattern. If we were to delete the information from the pixels containing the alien, we would also lose information from the intended Bragg peak measurement.

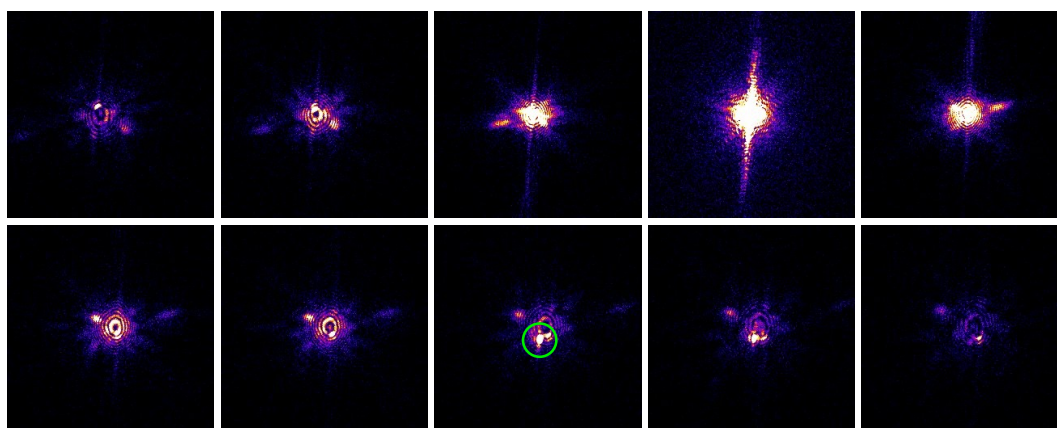


Figure 1.3 Snapshots from the rocking curve collection of a 3D Bragg peak. An alien containing extra information from another grain can be observed as a bright spot progressing from the upper left to the lower right through these frames. It is most noticeable where it is circled in green, flaring up as a bright spot after the main Bragg peak has already decreased in brightness.

A new scan from another Bragg angle requires more time and may meet with a similar problem. Furthermore, for certain techniques, at least three independent Bragg peak measurements from a single crystal are necessary [2]. Reducing the overall occurrence of aliens with our sample design is therefore preferable. The ideal sample would be an easily locatable, isolated grain. The isolation would ensure that information from nearby grains will not pose an issue to data collection while easily finding the same grain would allow us to collect multiple Bragg peaks from different angles. However, a single grain does not allow us to measure strain across a grain boundary. Thus, for our experiment, we designed a sample of isolated gold nanoparticles to allow grain boundaries to form within some particles while still facilitating the relocation of a single particle and the collection of uncontaminated diffraction data.

1.4 The Radiation Pressure Problem

Another major problem with collecting reliable diffraction data is the possibility of the particle rotating out of the Bragg condition during collection of the peak. The rocking curve for the frame-by-frame collection of the 3D diffraction pattern takes several hours during which the measured particle must be exposed to the high-powered x-ray beam. As shown in Figure 1.4, we observed significant drift in some of the diffraction patterns during collection from the gold nanoparticles when using earlier samples with silicon or sapphire substrates. This told us that the particle being measured rotated out of the Bragg condition over time due to the effect of the x-ray beam. This phenomenon has also been observed by other researchers at beamlines with increased x-ray flux [6, 10].

This rotation of the particle is caused by the radiation pressure of the high-powered x-ray beam which we use. Radiation pressure is proportional to the number of photons per second and inversely proportional to wavelength and acts perpendicular to the crystal lattice (See Figure 1.5). Thus, it follows that increased x-ray flux at higher energies increases the likelihood of nanoparticle rotation.

The monochromator at the 34ID-C beamline, which we use for our diffraction measurements, can access x-ray energies from 6-20 keV which corresponds to x-ray wavelengths of 0.06-0.2 nm [11]. Given these beam parameters and the small mass of the gold nanoparticle, if the particle is not firmly affixed to the substrate, the radiation pressure can exert a large enough force to cause the observed rotation of the nanoparticle.

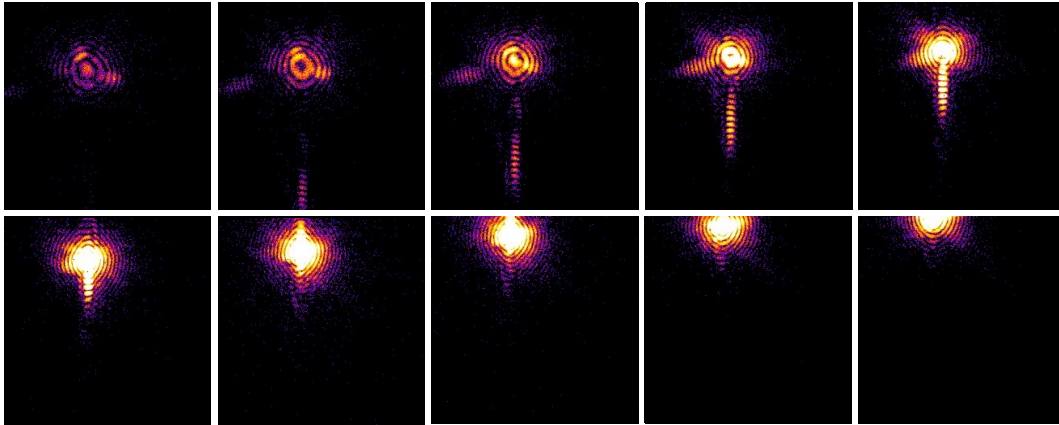


Figure 1.4 Snapshots from the rocking curve collection of a 3D Bragg peak showing an incomplete diffraction pattern in 3D reciprocal space for a rotating gold nanoparticle. This highlights the negative effect of a particle's motion on gathered diffraction data.

A strong enough force connecting the particle to the substrate must provide the resistance to this type of motion if we are to collect the entire Bragg peak without affecting the orientation of the particle. A robust sample is therefore defined by this condition. Hoping to produce stronger sample-substrate connections, we chose strontium titanate (SrTiO_3) as the substrate for our new gold nanoparticle samples because it has a more similar crystal structure to gold than silicon or sapphire. Both gold and strontium titanate have cubic lattices with similar parameters. Meanwhile, sapphire has a hexagonal crystal lattice, and silicon, while cubic, has a higher lattice parameter than gold. SrTiO_3 has also demonstrated high-quality interfaces with other materials due to its surface properties [12].

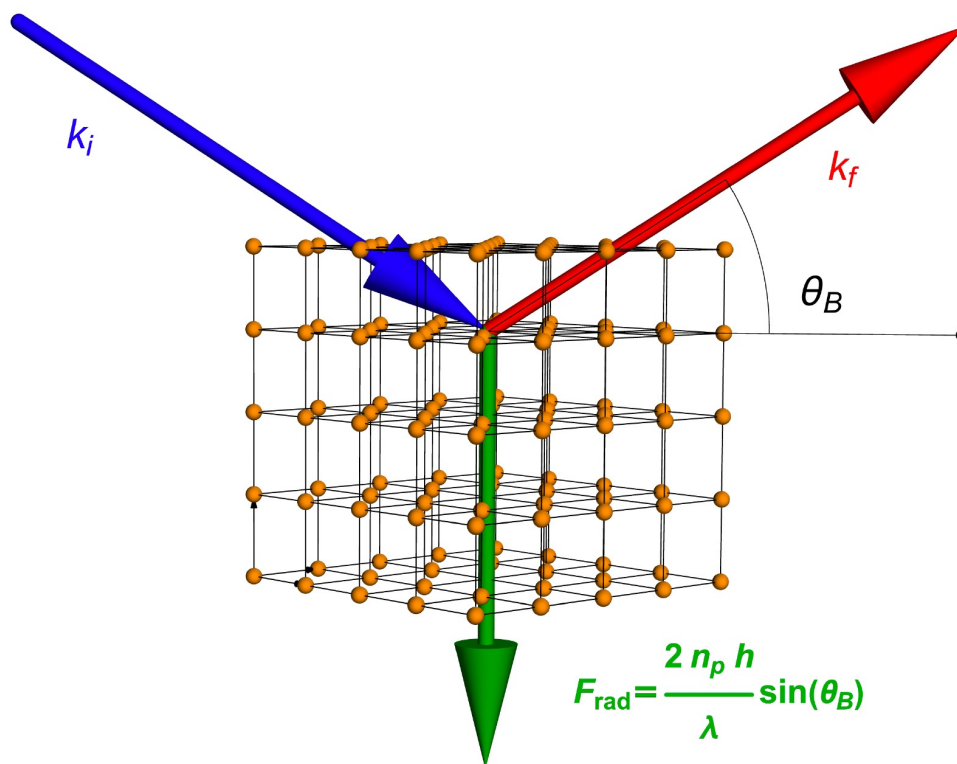


Figure 1.5 “Radiation Pressure” or the force caused by the change in the x-ray’s momentum (shown here as Δk), is exerted on the grain perpendicular to its crystal lattice with magnitude described by the equation in green, where n_p is the number of photons per second, h is Planck’s constant, λ is the x-ray wavelength, and θ_B is the Bragg angle. If not fixed securely in place, this force could cause the particle to rotate.

1.5 Finding Grain Orientations

The need for *a priori* information about a sample before applying coherent imaging phase retrieval algorithms has been well established [13–15]. In our case, we mostly depend on knowing the approximate orientation of the crystal before we arrive at the beamline to help us know where to look for the crystal’s Bragg peak. To gather this data, we use a Scanning Electron Microscope to perform Electron Backscatter Diffraction (EBSD) analysis on our samples before we take them to the beamline. This technique, shown in Figure 1.6, uses a focused beam of electrons to gather electron diffraction data from a single point on the surface of a sample. It then matches the bands

of the diffraction pattern to known crystal orientations for the material in question. Each point is then assigned a color corresponding to the best matching crystal lattice orientation for the collected pattern. The results can then be displayed as a colored grain orientation map.

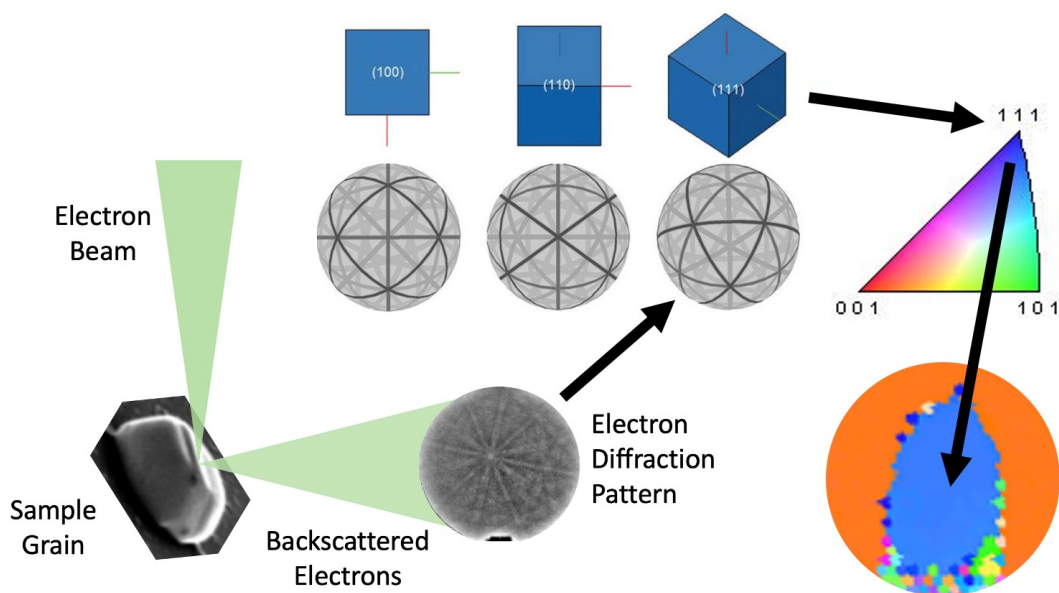


Figure 1.6 Schematic of the process whereby EBSD determines the orientation of grains in our gold nanoparticles. The uppermost graphic with the blue boxes representing cubic lattice orientations and their corresponding spherical diffraction patterns is from Oxford Instruments [16].

The orientations provided by this technique save us time and effort at the beamline by allowing us to quickly locate Bragg diffraction peaks. Although efforts are being made to develop an in situ method for grain orientation measurements based on Laue diffraction [11], this remains our standard operating procedure for now. The biggest challenge to the collection of EBSD data is charging of the sample. Sample charging is important to avoid because a buildup of electrons in an area of the sample can result in pattern distortions to the point where they are no longer useful in determining the grain orientation at that point [17]. Extensive charging often results in colorful but mostly meaningless EBSD scans (see Figure 1.7).

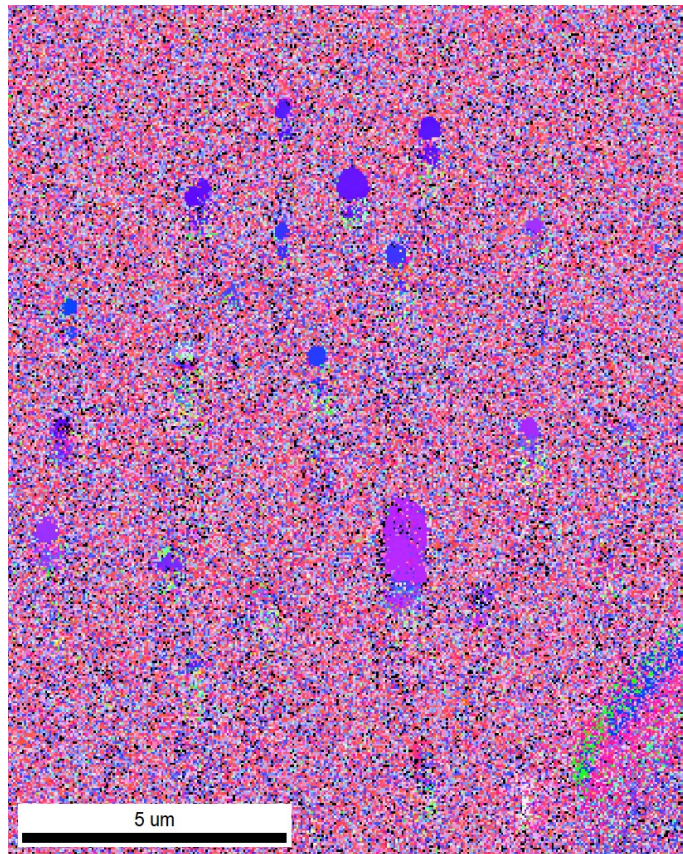


Figure 1.7 An EBSD scan of gold nanoparticles on a silicon substrate showing charging effects. When the software cannot match the pattern very well, it still makes its best guess which results in the colorful "Christmas lighting" observed here. Some gold nanoparticles have been lost in the background noise.

EBSD should be able to reach resolutions better than $0.1 \mu\text{m}$ in ideal conditions [17]. Because we want to measure the orientation of grains as small as 30 nm , we are already pushing the limits of the instrumentation. An insulating substrate such as sapphire can lead to a buildup of charge which further limits the resolution. To avoid this, we chose a conductive substrate for our gold nanoparticles, namely niobium-doped strontium titanate ($\text{Nb}:\text{SrTiO}_3$), to create a pathway allowing electrons to escape as current. This allows us to avoid charging defects so we can obtain more accurate *a priori* grain orientation information concerning the gold nanoparticles.

Chapter 2

Methods and Sample Recipe

In this chapter, I will describe the design and fabrication of our current samples of gold nanoparticles in isolated patches on a niobium-doped strontium titanate substrate. The main processes involved in their fabrication are photolithography, thermal deposition, and annealing. I will include standard operating procedures for each of these processes which have allowed us to produce repeatable results.

2.1 Sample Design

In the interest of creating isolated nanoparticles with easily identifiable positions, we designed our own photolithography mask . As will be explained in more detail in the next section, a mask is necessary for photolithography to select the areas which will be developed. In other words, the design of our mask directly transfers to the design of our sample. Based on what worked well with previous samples, our mask contains microscale square patches with various sizes and spacings and rows of lines with different widths and lengths. Number and letter labels are present throughout to make positions easily identifiable (see Figure 2.1). To design this mask, I used the open software package, KLayout [18].

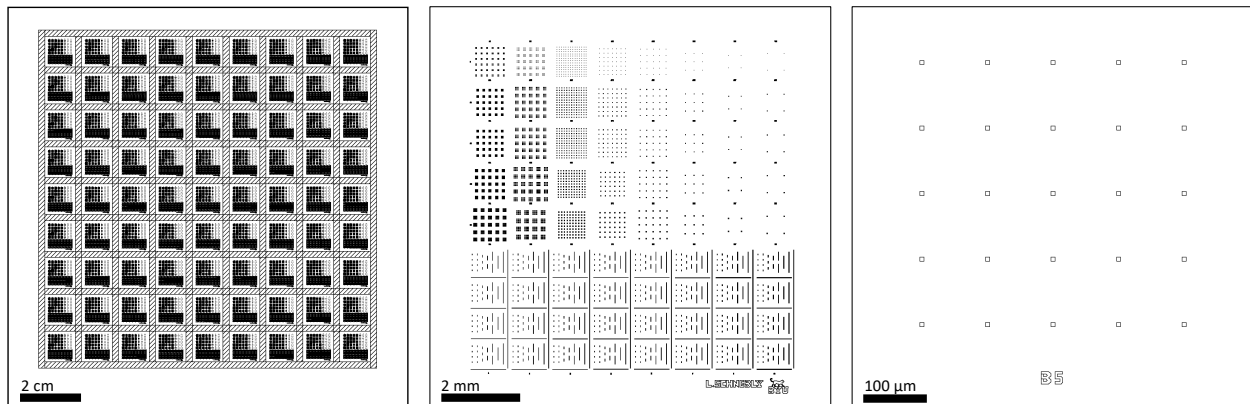


Figure 2.1 The features of this mask design directly correspond to our desired sample features of isolated gold patches. Here it is shown as displayed in KLayout [18] at various magnifications. The 5x5 in glass mask plate was coated with chromium everywhere except for where these shapes are placed.

If you are just getting started with KLayout, there are a number of helpful tutorials for designing a mask using this software. I have included some links which I found helpful from the University of Waterloo's Quantum-Nano Fabrication and Characterization Facility [19] and the University of Washington's Nanofabrication Facility [20]. They can help you install the correct software, set up your file, get started with different shapes, and teach you how to create arrays for a repeated design. For our mask design, you shouldn't need much training beyond this, especially if you are editing a previous mask design or template.

Once your design is completed, you will need to send the file along with an order form to Joe Bussio of the Electrical Engineering department. He will be able to create the mask using the Heidelberg DWL 66FS laser mask writer located in the BYU cleanroom. For the feature sizes which we have (down to $1\mu\text{m}$), we need to use the 2mm write-head, which should be able to achieve feature sizes down to 600nm. The biggest problem we faced with the mask design was a "dimensionless" error when the file was opened on the Heidelberg mask writer. This error was caused by not properly flattening all of the cells. As you create cells and copy them in an array, they form a hierarchy in the cell tree underneath the "TopCell." To collapse them, simply select the

"TopCell" and go to Edit > Cell > Flatten Cell. Tell it to flatten "All hierarchy levels" and to "Prune" all cells no longer being used. Once the process runs, you should see the cell tree has collapsed into a single instance of the "TopCell."

2.2 Photolithography

Photolithography is the process which allows us to transfer our designed pattern of microscopic features to a real sample. It uses ultraviolet light to weaken or strengthen a chemical layer, called a photoresist, which is applied in a uniform coat on the substrate's surface. The type of photoresist determines the reaction that will occur when it is exposed to UV light. The chemical bonds in a positive photoresist weaken with exposure to UV light while the bonds in a negative photoresist are strengthened when exposed to UV light. The practical differences can be summarized with the acronym NESPEG: for **N**egative photoresist, the areas **E**xposed to UV light **S**tay after development, and for **P**ositive photoresist, the **E**xposed areas **G**o.

For our sample recipe, we use the positive photoresist, AZ-3330. This is why our mask described in the last section was designed to have chrome everywhere except for where the shapes allow light to pass through. In this way, our mask selects the areas where light is able to affect the photoresist. Where the light passes through our mask to the sample surface, it weakens the chemical bonds of the AZ-3330 positive photoresist. When we develop the sample after exposure, these weakened areas of photoresist are easily removed, leaving areas where the substrate is exposed (see Figure 2.2). These areas correspond to the desired microscale features in our design and are where our gold nanoparticles will grow. A full standard operating procedure detailing our specific steps for performing photolithography on a 1x1 cm Nb:SrTiO₃ sample can be found in Appendix A.

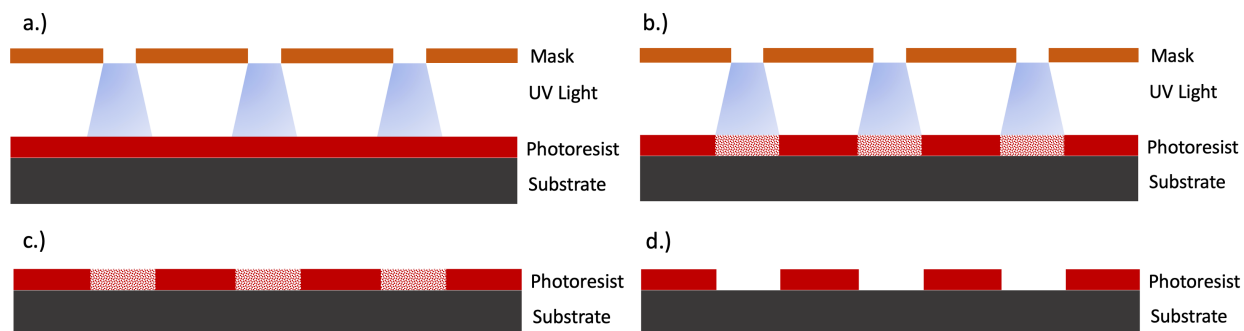


Figure 2.2 Schematic of photolithography. a.) The mask selects the areas through which light can pass through to the sample. b.) Where the light interacts with the AZ-3330 positive photoresist, the chemical bonds weaken. c.) We remove the weakened areas using the AZ-300 developer solution. d.) We are left with a microscale pattern of exposed substrate areas.

2.3 Thermal Deposition

Thermal deposition is the process whereby we deposit a thin film of gold onto the substrate we have just prepared with photolithography. It is achieved by heating a source material until it evaporates and allowing the resulting vapor to condense onto a substrate and form a thin film. We used the system in the basement of the Eyring Science Center, known as JIM, which allowed us to perform this deposition in a vacuum. The low pressure allows for the evaporation of gold at much lower temperatures.

For the setup, we placed gold beads in a molybdenum sample boat connected to an electrical circuit allowing us to control the temperature via the current. We mounted our sample to a plate suspended over the boat and placed the shutter, used to regulate the deposition rate and minimize contamination, at 1.5 inches from the top of its mounting pole. We then started the pump-down procedure to bring the system to a vacuum pressure of 6.2×10^{-5} Torr. Under vacuum, we incrementally increased the voltage until the sensor detected a rate of deposition. We started to see deposition at 90 V and at 120 V, we observed a deposition rate of 0.6 \AA/s . At 125 V it reached a steady 1 \AA/s deposition rate and we allowed the deposition to continue until the sensor indicated 125 \AA .

The following settings were recorded during our run:

Pressure: 6.2×10^{-5} Torr	Tooling Factor: 62%
Au density: 19.0	Z-ratio: 0.381
Evaporation Rate: 1 \AA/s	Voltage: 125 V
Film Thickness Readout: 125 \AA	

The result is an approximately 30 nm thick gold film across the entire surface of our sample. This thickness is different from our sensor readout because of the effect of the shutter. The resulting 30 nm thickness was verified using ellipsometry, which uses the change in a beam of polarized light to provide highly sensitive and accurate measurements of thin films. Following the deposition of the thin film, we used NMP to remove the rest of the photoresist layer along with the gold deposited on top of it. This left our sample with a thin gold film only in the areas where the substrate was exposed after photolithography (see Figure 2.3).

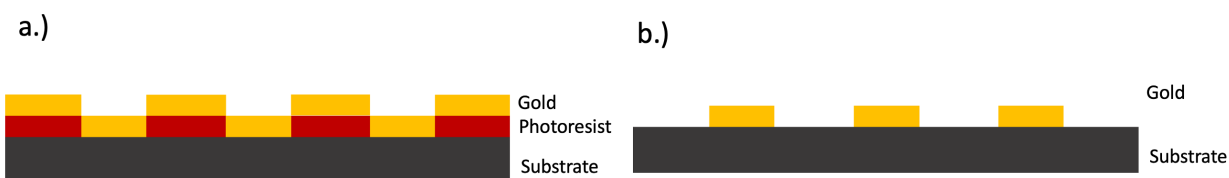


Figure 2.3 a.) Thermal deposition deposits a 30 nm thin film of gold as a blanket layer on our sample. b.) We remove the rest of the photoresist by developing with NMP leaving gold patches only in the desired areas.

2.4 Annealing

Annealing is the heat treatment process whereby we go from a thin gold film to gold nanoparticles. For this process, we use one of the Chemical Vapor Deposition (CVD) furnaces owned by the Nanomaterials Research Group at BYU. Usually, these furnaces are set up with different gas flows,

but we anneal our samples in an atmosphere of ambient air because we only need the heating capacity. We simply place our samples in the center of a glass tube that is open at both ends.

Kovalenko, et. al, recorded that annealing a lithographically patterned gold sample in ambient air at 1173 K for 24 hours resulted in agglomeration of the patterned film and formation of faceted gold particles [21]. We patterned our recipe after these findings and heat our samples during annealing to 900 °C and hold them at that temperature for about 20 hours. The mentioned agglomeration of the gold thin film into droplets is called dewetting and is driven by the minimization of surface energy. When gold dewets, it forms into beads that migrate across the surface leaving behind bare areas. In this way, the process of dewetting provides the means to transform a flat film of gold into isolated nanoparticles (see Figure 2.4).

After sufficient time has been given for the gold to dewet, we allow the samples to cool slowly until they return to ambient temperatures. This slow cooling process takes about 6 hours during which the nanoparticles recrystallize. Recrystallization describes the process whereby the gold atoms reorganize themselves into crystal lattices as they solidify. Cooling the grains too quickly can lead to more chaotic grain structures while letting them cool slowly allows the atoms to reach an ordered crystal lattice structure which minimizes energy and strain. That this occurs will be shown in the next chapter when we discuss the clean, faceted grains which we have observed.

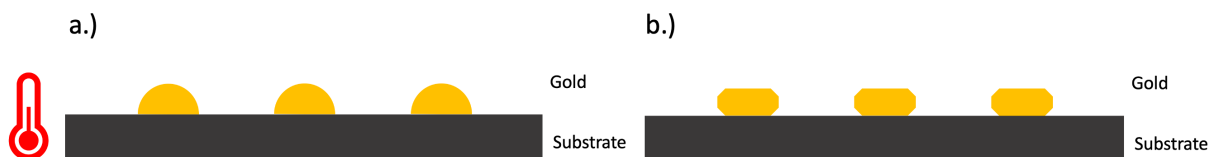


Figure 2.4 a.) Annealing at 900 °C causes the gold to dewet and form beads on the substrate. b.) Allowing the sample to cool slowly allows recrystallization of the gold to form faceted nanoparticles.

Chapter 3

Results

In the results chapter, I will present data which show why our sample recipe is ideal for 3D strain-mapping experiments at high-energy x-ray beamlines. Specifically, I will highlight how the sample characteristics of isolated patches of faceted particles, a conductive substrate, and a robust sample-substrate interface directly combat the three main challenges observed with previous samples: aliens, charging, and drift.

3.1 Isolated Patches of Faceted Particles

The isolated patches of faceted gold nanoparticles we can repeatedly obtain with our sample recipe greatly reduce the occurrence of aliens, as described in Sec. 1.3. This is because the patches and lines were designed to have a median spacing of $100\ \mu\text{m}$ between them. The particles within a patch also have space between them on the order of the particles themselves as a result of dewetting (see Figure 3.1). In addition to allowing us to scan a Bragg peak without alien contamination, these spacings also allow us to more easily identify the position and orientation of a single grain so we can locate its Bragg peak in detection space. Being able to quickly relocate a particle on our sample also allows us to easily collect multiple Bragg peaks from a single grain.

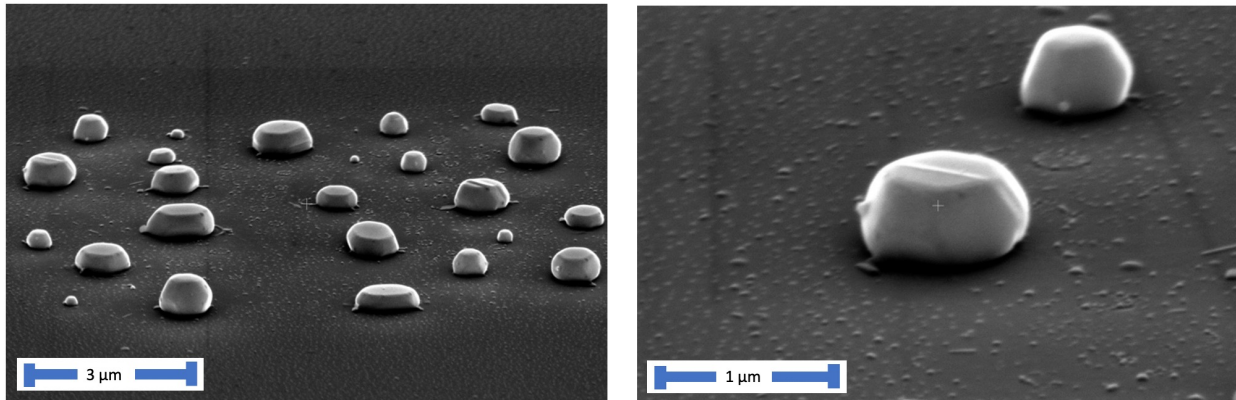


Figure 3.1 SEM images showing the submicron faceted gold nanocrystals which we obtain with our recipe. Note the spacing between particles is on the order or larger than the size of the particles themselves allowing us to more easily distinguish between grains.

The faceted grain growth observed is a sign of ordered crystal lattices. We have found that the nanoparticles tend to preferentially orient their crystal lattices in the $[111]$ direction, but that particles containing twin grain boundaries are also fairly common, with one or two present in most of our patterned patches. Twin grains have the same crystal structure but are oriented differently in space (see Figure 3.2). Most importantly, the twin boundary represents a common plane of atoms between the two grains. Because of this ordering, twin grain boundaries provide an ideal environment for us to measure the strain across a grain boundary.

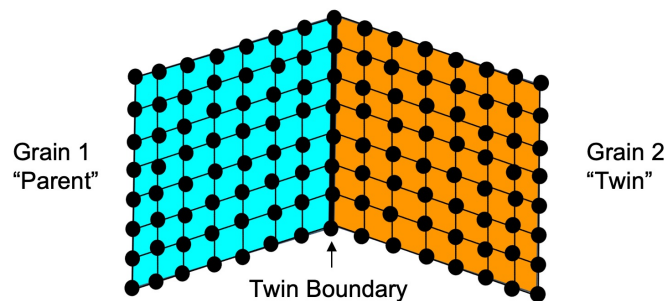


Figure 3.2 Schematic representation of a twin grain boundary. The atoms of the twin grain can be generated from the atoms of the parent grain by reflection across the common plane of their twin boundary.

3.2 Conductive Substrate and EBSD

The conductive properties of our substrate, niobium-doped strontium titanate, mitigate the effects of charging observed in past samples with substrates such as sapphire (see Figure 3.3). As discussed in Sec. 1.5, charging was the main barrier to gathering reliable orientation data from our samples prior to beamline experiments because the buildup of charge negatively impacted EBSD analysis in a Scanning Electron Microscope. Our new conductive substrate has reduced charging effects, allowing clear measurement of the orientation for each grain. Because of this, we have been able to use EBSD to identify many prime sites for lensless imaging. Our current operating procedures for EBSD analysis of an area of gold nanoparticles can be found in Appendix B.

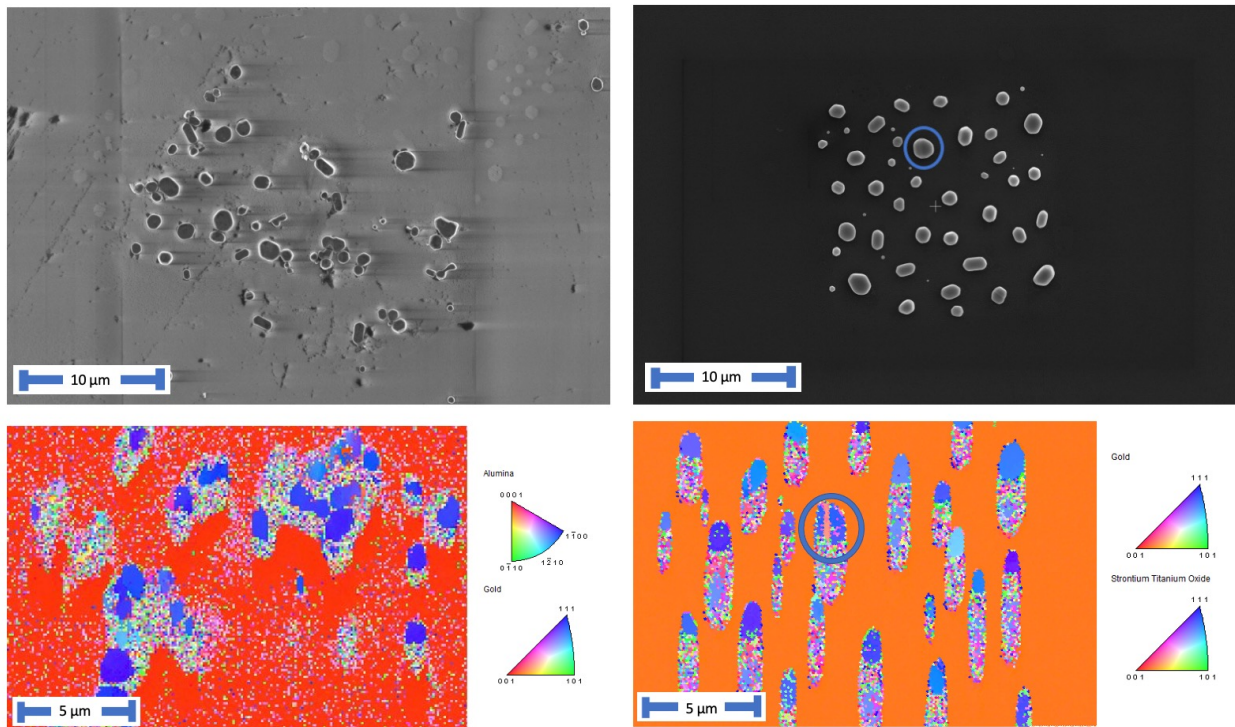


Figure 3.3 SEM images and EBSD Inverse Pole Figure (IPF) Maps for an old sample with a sapphire substrate (left) and a newer sample with a Nb:SrTiO₃ substrate (right). Here, it is shown that the effects of charging in the SEM are less severe for a conductive substrate. Note the circled particle and its "sandwich" twin boundary. We identified this particle as an ideal candidate for measurement of a grain boundary.

3.3 Twin Grain Reconstruction

The successful reconstruction of multiple sets of twin grains shows that the Au/Nb:SrTiO₃ sample-substrate interface is robust enough to counteract the effects of radiation pressure described in Sec. 1.4. The robust qualities of our sample recipe are best demonstrated by the absence of particle drift and rotation in the new samples. We have been able to consistently collect clean diffraction patterns which have yielded viable reconstructions using the algorithms mentioned in Sec. 1.2. Specifically, we have seen improvement in the reconstruction of grains on either side of a twin boundary, with little to no missing information between the grains (see Figure 3.4).

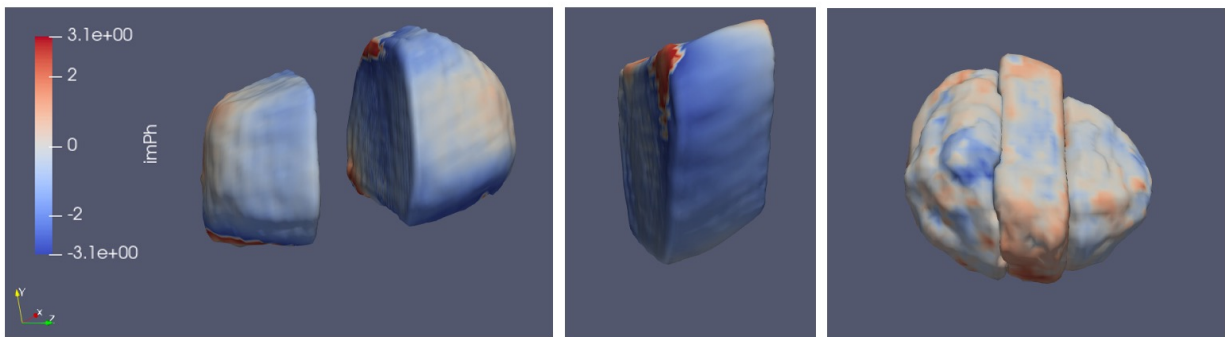


Figure 3.4 3D strain map of the twin grain particle circled in blue in Figure 3.3. The reconstructions for the parent and the twin were produced from separate x-ray diffraction patterns using Cohere [3]. From left to right: the parent grain, the twin, and the two reconstructions overlaid.

Aside from the similarities in crystal structure and its proven aptitude for thin films mentioned in Sec. 1.4, we have little explanation for why the Au/Nb:SrTiO₃ sample-substrate boundary has yielded better results than previous samples. Preliminary SEM analysis using backscatter electron imaging and Energy-Dispersive Spectroscopy (EDS) of the bonding sites between the gold particles and the Nb:SrTiO₃ substrate may indicate that the gold particles become at least partially embedded in the substrate during the annealing process.

3.4 Conclusions

Isolated patches of gold nanoparticles are ideal for lensless x-ray imaging. Niobium-doped strontium titanate has been shown to be a promising substrate for these patches of gold particles because it is a single-crystal, conductive substrate that prevents the rotation of the particles due to radiation pressure. Preparing samples with photolithography allows us to vary the size and spacing of the Au particle patches on Nb:SrTiO₃. Thermal evaporator deposition gives us control over the thickness of the deposited gold layer. Annealing causes the gold to dewet and form faceted gold particles that are around a micron or less in size. The conductive properties of Nb:SrTiO₃ allow us to easily collect EBSD data about the orientations of crystals in a patch to easily determine grain orientation and identify prime sites such as twin grain boundaries. Using x-ray radiation from the Advanced Photon Source, we can then find and scan multiple Bragg diffraction peaks from a single grain. Reconstruction algorithms allow us to achieve nanometer-scale strain imaging from these collected scans. We have successfully reconstructed multiple sets of twin grains from the sample fabricated with the described recipe showing that it is well suited for lensless 3D strain mapping experiments at high-energy x-ray beamlines.

Appendix A

Photolithography on Nb:SrTiO₃ Standard Operating Procedures

Materials brought to the BYU cleanroom:	Materials in the BYU cleanroom:
* 1x1 cm Nb:SrTiO ₃ sample(s)	* throwaway silicon wafer
* sample tweezers	* wafer tweezers
* super glue	* HMDS primer agent
* ruler	* AZ-3330 positive photoresist
* fine-tipped permanent marker	* Laurell spin coater
* photolithography mask with clear features	* hot plate
	* MA150 Karl Suss Aligner
	* AZ-300 developer solution

1. Attach the 1x1 cm Nb:SrTiO₃ sample(s) to the throwaway silicon wafer:

- Use the ruler and the fine-tipped permanent marker to make straight lines where you want the samples to go. Make these lines parallel to the flat edge of the silicon wafer. This will make it easier to align later. If doing more than one Nb:SrTiO₃ sample, make

sure they are placed exactly 1.4 cm apart vertically or horizontally to line up with the mask.

- Add a small dot of super glue near the center of each sample and carefully drop it into place using the sample tweezers.
- Let the super glue dry until the Nb:SrTiO₃ sample no longer moves when gently nudged with the tweezers. Putting it on the hot plate can speed up the drying process.
- If any super glue gets on the surface of the sample, wet a Kim wipe with acetone and carefully remove it.

2. Plasma clean the sample for 1 minute using the plasma cleaner in the BYU cleanroom:

- Plasma cleaning removes any excess surface gunk (especially hydrocarbons from fingerprints, etc.)
- The plasma cleaner is located in the white light area of the cleanroom on the back (west) wall.
- Follow the instructions as posted near the machine. Start the timer once you strike the plasma.

3. Apply the Photoresist:

- Center the wafer on the spinner and turn on the vacuum.
- Select Program 12 (5000 rpm, 1 min) – the settings for the "Davis Group"
- Select "Run Mode"
- Apply 5 drops of HMDS to each 1 cm sample. Immediately after doing so, close the lid and press "run." Waiting too long will cause it to spread and dry unevenly.
- Apply 15-20 drops of AZ3330 to each 1x1 cm Nb:SrTiO₃ sample. Immediately after doing so, close the lid and press "run."

- Check to make sure the coat of AZ3330 has covered the entirety of the sample(s). A little waviness is not bad but use your best judgment. If it looks too messy, clean it off with acetone on the other spinner around the corner. Then go back to step 2.
- If you are satisfied, place the sample on the hot plate and do a pre-exposure bake at 90 °C for 1 minute.

4. Photolithography Light Exposure:

- Edit the program before loading the sample. Usually, you will need to click "Return" then "Change Program" and "Edit." You do not need to "Save" the program.
- Select the following settings:

Very Important:	Less Important: (recorded here only for consistency)
<ul style="list-style-type: none"> * Exposure Time: 25.0 s * Alignment Gap: 50 μm * Resist: Positive * Mode: Manual Align * Align. Check: On 	<ul style="list-style-type: none"> * Max Exposures: 500 * Exposure: 9 * Max Contacts: 100 * Contact: 0 * Soft C Delay: 10 s * WEC: Contact * Prealigner Type: o * Mic/Mask Teach: Default * Data Logging: ON

- Once these settings have been selected, press "START" to begin processing wafers.
- Load the wafer. You want the Nb:SrTiO₃ sample edge to be straight in line with the mask. If you made sure the Nb:SrTiO₃ sample edge was parallel to the flat edge of the

silicon wafer, you can line up the silicon straight edge with the mark on the disk holder.

- Turn on the vacuum and press "Continue."
- Load the mask. Use the one with clear features (blank where we want patches of gold and chrome elsewhere). You should load it with the shiny side facing up. If placed the wrong way, the reflections will create ghost images. For the current mask, shiny side up makes all the letters backward, but the rest of the features turned out as desired. Hopefully, we can fix the backward lettering with a new mask in the future.
- Once the mask is in place, turn on the vacuum and then the clamps.
- Next, the machine should allow you to align before exposure. You will need to select the "Mask" button on the left joystick and the left button on the right joystick (I don't remember the label).
- You should be able to see the 1cm square sample under the mask. Move the mask so the 1 cm sample lines up with one of the 1 cm squares on the mask. I usually don't need the microscope screen to do this.
- I am not sure why this is sometimes a problem and other times not, but if you notice that the mask has been pushed out of the grip of the vacuum by the sample, exit the program, and try again with the alignment gap set to 550 μm . This accommodates the 0.5 mm width of the Nb:SrTiO₃ sample.
- Once you have the mask aligned where you want it, deselect the lit-up buttons on the joysticks. The green "Exposure" button should now be lit. Press it once. It will then ask you to confirm the alignment again which you do by pressing the "Exposure" button a second time.
- The microscope will raise, and the light will move forward and expose for 25 seconds. Do not look straight at the light.
- When it is done, unload the mask and the sample.

5. Develop the Pattern:

- Place the sample on the hot plate for a 1-minute post-exposure bake at 90 °C.
- Place the wafer into the development holder (which looks like a plastic arrow) and slide down the tab to hold it in place.
- Check the AZ-300 developer solution. If it is too dark in color, you can pour it into the waste container and replace it with new solution. Make sure to check the label to make sure it is the correct chemical to develop AZ-3330.
- Submerge the wafer in the solution and agitate slightly for 30 seconds.
- Rinse with deionized water and use compressed air to sheet off the water so it does not dry on the surface.
- Check the pattern under the optical microscope in the NE corner.
- If not sufficiently developed, submerge it again in the solution for an additional 30 seconds. Repeat the development and check cycle until the pattern is sufficiently developed. For the most recent sample, I only had to do the first 30 seconds.
- If the pattern was not aligned correctly, if you overdevelop, or if there is something else wrong with it, you can still rinse off the photoresist with acetone on the spinner and go back to step 2. You can also develop it for longer if the acetone doesn't work completely. But end with acetone before the plasma clean.
- If the pattern developed correctly, you are done with the photolithography!

Appendix B

EBSD of Gold Nanoparticles Standard Operating Procedures

Preparation:

- Sample needs to be clean prior to imaging to obtain good EBSD data.
- The operator should be trained on using the Apreo SEM and EBSD process and software.
- To maintain cleanliness of sample wear gloves and avoid touching the face of the sample to be imaged even with gloves or tweezers.
- The microscope should be scheduled for your use. One scan typically takes about 1 hour.

Procedures:

1. Getting started:

- Microscope should be logged in and the software up and running. If not or if there is an error message, contact Mike to correct the problem.

- Check the vacuum status (column icon on bottom of the screen should be all green) and the gun emission (green bar under the BEAM ON button). If either of these are not green then contact Mike

2. Loading and Positioning the Sample:

- Open the chamber by pressing the vent button and confirming the vent.
 - If the chamber fails to vent after several minutes (watch the green progress bar on the bottom of the screen) contact Mike to replace the N₂ gas cylinder.
- Wear powder-free nitrile gloves when directly handling microscope parts or samples. Gloves are available in rooms 106 and 109.
- Mount sample on microscope stub using carbon tape
- Place the mounted sample in one of the appropriate positions on the sample holder in the microscope.
 - For EBSD, the best location is either of the two holes closest the slanted part of the stage opposite the part of the stage which sticks up in a point.
 - The stage will also need to be rotated so that the slanted part of the stage (where the samples are loaded) is on the right side when the chamber is opened (left side if looking at the CCD camera). Because the microscope's perpendicular "zero" position is at -33 degrees, this desired position corresponds to 147 degrees rotation.
 - Make sure all of the samples being placed in the microscope are approximately the same height (within 1-2 mm)
 - Sample positions for EBSD are secured by a spring (some other locations are secured using a set screw and are labeled with the word screw).
 - Make sure the sample is pushed securely down into the hole.

- Ensure the Sample will not hit the pole piece
 - Make sure the CCD image is not paused
 - Slowly close the door and carefully watch that your sample stays below the 10 mm marker on the image
 - * If the top of the highest sample appears to be above the 10 mm marker on the image open the door and lower the stage.
 - Select the navigation panel.
 - Adjust the z value to a lower number until you are sure the top of the sample will not be above the 10 mm marker. (for EBSD you want an extra 5 mm)
- Select the “take nav-cam photo” box to take a new nave-cam photo. (This can be done afterward if necessary)
- Press the Pump button and then select the “No Accessory” item from the pop-up window. None of these accessories are used for EBSD.
- While the chamber is pumping down, select the following parameters:

* KV: 20 kV	* Use Case: Standard
* Probe current: 1.6 nA	* Detector: ETD
* Dwell Time: 100 ns	* Live imaging
* Image Resolution: 1536 X 1024	

3. Find Area of Interest and Focus:

- Select the area on a sample you want to start with by double clicking on the area of interest on the nav-cam photo.
- When the chamber has finished pumping down to vacuum the BEAM ON button will become available and the column icon on the bottom of the screen will be green again.

Turn on the electron beam by clicking on the BEAM ON button.

- Un-pause the image and adjust the brightness and contrast using the knobs on the controller (the oscilloscope looking feed can be used to ensure image is not being washed out) a brightness of around 42% is usually desired.
- Focus the image using the focusing knobs on the controller and link the Z to FWD.
 - Find a reasonable focus at low magnification first
 - Once a reasonable focus has been obtained, increase magnification to 2,000X and refocus until you are reasonably well focused.
 - Link Z to FWD
 - Bring the sample up to **15 mm** using the Z access control. Note: This is different from the standard procedure for imaging that is not accompanying EBSD.
 - Re-focus the image and relink the Z to FWD.

4. Position Sample for EBSD

- Make sure Y-Z link is checked on the navigation panel.
- Tilt the sample to 45 degrees and make sure it is not in danger of hitting the pole piece. (Lower the stage Z if it looks like the sample may hit the pole piece.)
- If it is safe, tilt the sample to 70 degrees
- Refocus as needed
- Check the “dynamic focus” on the navigation panel and make sure the angle indicated matches the stage tilt angle.
- Drive stage to relocate area of interest if needed.

5. Set up the EBSD detector

- Insert the detector, watching to make sure it won't hit the stage or sample. Keep your finger on the button the entire time so you can stop it immediately if anything is wrong.
- Pause the CCD camera on the microscope.
- Start the EBSD program called OIM DC located on the left secondary screen. (Once the program starts you will have to use the second keyboard and mouse to your left when using the second screen)
- Select 8x8 binning on the Camera tab of the camera controls.
- Make sure "Double Clock" is checked on the Camera tab.
- Make sure the subtract background and any other checked boxes in the image processing box on the image processing tab of the camera controls are unchecked.
- On the camera tab, adjust Exposure to the highest it can go without reducing the frames per second (for 8x8 binning this is at 8.1, max fps is 123.4) and then adjust the Gain to get a camera image just below saturation. (Make sure to keep gain below 800, ideally below 600. If you cannot, adjust the voltage and refocus.)
- Check the dynamic background subtract box in the image processing tab. This will apply a Gaussian subtraction to reduce background noise. We do not capture a background for gold on Nb:SrTiO₃ because we still want the single-crystal substrate to index.
- Load the correct phase file(s) on the phase tab; for this sample select gold. Selecting strontium titanate is optional because of the similar crystal lattice parameters. Sometimes leaving it out seems to produce better results.
- Turn on the external control using the "Ext XY" toolbar button
- Set the working distance calibration on the toolbar drop-down to "15*mm"
- Capture an SEM image on the interactive tab

- Check the confidence index (CI) and fit on the interactive tab. Try clicking on different areas on the SEM image until you find a pattern near the center that seems to fit well and has reasonable confidence then click the "auto-tune calibration" toolbar button.
- If needed check the Hough Transform settings on the Hough tab.

6. Perform the EBSD Scan

- On the SEM Image on the Scan tab, Select the area you would like to scan by dragging a box that covers the area. It can then be edited to be a specific length and height.
- Select the location and file name to store the data on the dialog box that appears.
- Set the scan type as square because it is more compact (other option is hexagonal which works fine as well).
- Adjust the scan dimensions and start location if needed.
- Set the step size to 0.1 micron (10 nm). This seems to be as small as you can go without the scan taking really long or image drift becoming significant
- Estimate the scan time using the number of points and the current camera frame rate (you can just click on "estimate scan time" in the pop-up)
- Adjust the step size or scan dimensions to alter the scan time if necessary.
- Make sure the "save all patterns" checkbox is unchecked because it will generate much larger file sizes than we need.
- Click OK to close the dialog
- Click the "Start Scan" button to start the scan. It will let you know with a pop-up window when it is finished. (If you notice anything wrong after you have started, you can also stop the scan by pressing the abort button.)
- Save your work and any desired images to your

- EBSD scan files can be opened in the "OIM Analysis" software
- To generate IPF maps showing grain orientations, simply click on the toolbar option (looks like a colored triangle) once the scan has loaded.

7. Unload the Sample

- Release external control, un-pause the CCD camera, and extract the EBSD detector.
- Once the EBSD detector is fully retracted, return the stage to zero tilt.
- Press the vent button and confirm the vent.
- Remove samples using tweezers after the vent process has completed.
- Adjust the stage to 47 mm using the Z-axis control for the next person.
- Pump the chamber back to high vacuum by pressing the Pump button and selecting the "No Accessory" option from the popup window.

Bibliography

- [1] K. Lu, L. Lu, and S. Suresh, “Strengthening materials by engineering coherent internal boundaries at the nanoscale,” *science* **324**, 349–352 (2009).
- [2] M. C. Newton, “Concurrent phase retrieval for imaging strain in nanocrystals,” *Physical Review B* **102**, 014104 (2020).
- [3] C. Park, “Texture: Crystal Structure Analysis,” <https://ocw.snu.ac.kr/sites/default/files/NOTE/2019-XSA-18-texture-03-09.pdf> (Accessed March 2, 2023).
- [4] K. P. Shah, “The Handbook on Mechanical Maintenance,” <https://practicalmaintenance.net/?p=1618> (Accessed March 2, 2023).
- [5] M. J. Cherukara, R. Pokharel, T. S. O’Leary, J. K. Baldwin, E. Maxey, W. Cha, J. Maser, R. J. Harder, S. J. Fensin, and R. L. Sandberg, “Three-dimensional X-ray diffraction imaging of dislocations in polycrystalline metals under tensile loading,” *Nature communications* **9**, 3776 (2018).
- [6] A. Björling, L. A. Marçal, J. Solla-Gullón, J. Wallentin, D. Carbone, and F. R. Maia, “Three-dimensional coherent Bragg imaging of rotating nanoparticles,” *Physical Review Letters* **125**, 246101 (2020).

- [7] J. Miao, T. Ishikawa, I. K. Robinson, and M. M. Murnane, “Beyond crystallography: Diffractive imaging using coherent x-ray light sources,” *Science* **348**, 530–535 (2015).
- [8] B. Frosik and R. Harder, “Cohere,” <https://cohere.readthedocs.io/en/latest/>; <https://github.com/AdvancedPhotonSource/cohere> (Accessed March 2, 2023).
- [9] J. R. Fienup, “Phase retrieval algorithms: a comparison,” *Applied optics* **21**, 2758–2769 (1982).
- [10] M. Liang, R. Harder, and I. Robinson, “Radiation-driven rotational motion of nanoparticles,” *Journal of Synchrotron Radiation* **25**, 757–762 (2018).
- [11] A. Pateras *et al.*, “Combining Laue diffraction with Bragg coherent diffraction imaging at 34-ID-C,” *Journal of Synchrotron Radiation* **27**, 1430–1437 (2020).
- [12] D. Deak, “Strontium titanate surfaces,” *Materials Science and Technology* **23**, 127–136 (2007).
- [13] J. R. Fienup, “Reconstruction of a complex-valued object from the modulus of its Fourier transform using a support constraint,” *JOSA A* **4**, 118–123 (1987).
- [14] S. Marchesini, H. He, H. N. Chapman, S. P. Hau-Riege, A. Noy, M. R. Howells, U. Weierstall, and J. C. Spence, “X-ray image reconstruction from a diffraction pattern alone,” *Physical Review B* **68**, 140101 (2003).
- [15] A. M. Maiden and J. M. Rodenburg, “An improved ptychographical phase retrieval algorithm for diffractive imaging,” *Ultramicroscopy* **109**, 1256–1262 (2009).
- [16] Oxford, “Interpreting the Diffraction Pattern,” <https://www.ebsd.com/ebsd-explained/interpreting-the-diffraction-pattern> (Accessed March 2, 2023).
- [17] J. I. Goldstein, D. E. Newbury, J. R. Michael, N. W. Ritchie, J. H. J. Scott, and D. C. Joy, *Scanning electron microscopy and X-ray microanalysis* (Springer, 2017).

-
- [18] KLayout, “KLayout - Your Mask Layout Friend,” <https://www.klayout.de/> (Accessed March 7, 2023).
- [19] QNFCE, “KLayout Tutorial 0: Installation and Setup,” https://www.youtube.com/watch?v=WUEh_NahYGU&list=PL12BCN5zxKhysQPbl0Fy0a6x0fiCPJZB- (Accessed March 7, 2023).
- [20] WNF, “Some Basic Concepts of CAD for Nanostructure Fabrication,” https://ebeam.wnf.uw.edu/ebeamweb/training/cad_tut_main/cad_tut_prin/cad_tutorial_principles.html (Accessed March 7, 2023).
- [21] O. Kovalenko, C. Brandl, L. Klinger, and E. Rabkin, “Self-Healing and Shape Memory Effects in Gold Microparticles through the Defects-Mediated Diffusion,” *Advanced Science* **4**, 1700159 (2017).

Index

Index

Alien, 5, 17
Annealing, 15
Bragg Coherent Diffraction Imaging (BCDI),
3
Charging, 9, 19
Crystal lattice, 2
Dewetting, 16, 17
Electron Backscatter Diffraction (EBSD), 8,
19, 29
Grain boundaries, 2, 18
Mask, Photolithography, 11
Nb:SrTiO₃, 10
Photolithography, 13, 23
Photoresist, 13
Radiation pressure, 6, 20
Reconstruction, 20
Strain, 2
Thermal Deposition, 14